

Cholinergic Modulation of GABAergic and Glutamatergic Transmission in the Dorsal Subcoeruleus: Mechanisms for REM Sleep Control

David S. Heister, PhD; Abdallah Hayar, PhD; Edgar Garcia-Rill, PhD

Center for Translational Neuroscience, Department of Neurobiology and Developmental Sciences, University of Arkansas for Medical Sciences, Little Rock, AR

Study Objectives: Dorsal subcoeruleus (SubCD) neurons are thought to promote PGO waves and to be modulated by cholinergic afferents during REM sleep. We examined the differential effect of the cholinergic agonist carbachol (CAR) on excitatory and inhibitory postsynaptic currents (PSCs), and investigated the effects of CAR on SubCD neurons during the developmental decrease in REM sleep.

Design: Whole-cell patch clamp recordings were conducted on brainstem slices of 7- to 20-day-old rats.

Measurements and Results: CAR acted directly on 50% of SubCD neurons by inducing an inward current, via both nicotinic and muscarinic M1 receptors. CAR induced a potassium mediated outward current via activation of M2 muscarinic receptors in 43% of SubCD cells. Evoked stimulation established the presence of NMDA, AMPA, GABA, and glycinergic PSCs in the SubCD. CAR was found to decrease the amplitude of evoked EPSCs in 31 of 34 SubCD cells, but decreased the amplitude of evoked IPSCs in only 1 of 13 SubCD cells tested. Spontaneous EPSCs were decreased by CAR in 55% of cells recorded, while spontaneous IPSCs were increased in 27% of SubCD cells. These findings indicate that CAR exerts a predominantly inhibitory role on fast synaptic glutamatergic activity and a predominantly excitatory role on fast synaptic GABAergic/glycinergic activity in the SubCD.

Conclusion: We hypothesize that during REM sleep, cholinergic "REM-on" neurons that project to the SubCD induce an excitation of inhibitory interneurons and inhibition of excitatory events leading to the production of coordinated activity in SubCD projection neurons. The coordination of these projection neurons may be essential for the production of REM sleep signs such as PGO waves.

Keywords: Carbachol, subcoeruleus, rapid eye movement, whole-cell, PGO waves

Citation: Heister DS; Hayar A; Garcia-Rill E. Cholinergic modulation of GABAergic and glutamatergic transmission in the dorsal subcoeruleus: mechanisms for REM sleep control. *SLEEP* 2009;32(9):1135-1147.

RAPID EYE MOVEMENT (REM) SLEEP IS A DISTINCT HIGH FREQUENCY OSCILLATION AROUSAL STATE THAT HAS BEEN LINKED TO SEVERAL ASPECTS OF brain function including developmental maturation of the brain, modification of synaptic plasticity and memory formation, as well as regulation of metabolic functions.¹⁻⁵ A landmark study by Aserinsky and Kleitman first identified the REM sleep state.⁶ A substantial amount of subsequent research localized the generating mechanisms of this state to brainstem nuclei.⁷⁻⁹ Of particular importance are clusters of putative cholinergic neurons within the pedunculopontine (PPN) and laterodorsal tegmental (LDT) nuclei that have been characterized as "REM-on" neurons because of increased firing during REM sleep.^{10,11} The combined data obtained from in vivo, lesion, transection, and pharmacological studies have suggested that these putative cholinergic "REM-on" neurons in the brainstem are critically important for the generation and maintenance of the REM sleep state via widespread projections to the thalamus, brainstem, and specifically to the anterior pons.^{7,12-18} Anatomical studies described choline acetyltransferase-immunoreactive processes in the region of the anterior pons.¹⁹ Several early in vivo studies used injections of the nonspecific cholinergic agonist

carbachol (CAR) into the anterior pons to replicate the proposed downstream effects of PPN/LDT neurons. These injections induced a REM sleep-like state in cats, including muscle atonia and ponto-geniculo-occipital (PGO) waves. Lesions of this anterior pontine area could produce REM sleep without atonia or REM sleep without P-waves (the rat equivalent of PGO waves).²² Furthermore, afferents from the PPN/LDT to the cholinceptive pontine wave generating site in the rat have been described.²³ Recent in vivo studies were aimed at more precisely localizing the neurons affecting REM sleep signs. Using microdialysis injections and cell soma lesion techniques, several groups have shown that a small nucleus termed the dorsal subcoeruleus (SubCD) nucleus, also known as the sublateralodorsal nucleus, has a major role in the induction of several REM sleep signs.^{7,23-25} In addition, the use of c-Fos labeling has shown that the SubCD contains a population of "REM-on" neurons.²⁶ These anatomical and lesion studies have suggested that the SubCD plays a major role in the production of REM sleep state atonia via descending projections to the medulla and spinal cord.^{7,23-26} Additionally, there is evidence that the SubCD may also affect REM sleep processes via ascending projections to forebrain structures.^{27,28}

A recent comprehensive in vitro study of SubCD cells reported the presence of distinct populations of neurons that were either excited or inhibited by CAR, some of which had low-threshold spikes.²⁹ Histological analyses by several groups have shown this nucleus to consist of a mixture of mostly GABAergic and glutamatergic neurons.^{23,24,30} We recently described the presence of electrical coupling and spikelets in the SubCD and provided evidence of electrically coupled neurons in both the PPN and SubCD.^{31,32} The present investigation of the SubCD

Submitted for publication January, 2009

Submitted in final revised form February, 2009

Accepted for publication April, 2009

Address correspondence to: Edgar Garcia-Rill, PhD, Center for Translational Neuroscience, Department of Neurobiology and Developmental Sciences, University of Arkansas for Medical Sciences, 4301 West Markham St., Slot 847, Little Rock, AR 72205; Tel: (501) 686-5167; Fax: (501) 526-7928; E-mail: garciarilledgar@uams.edu

consists of an examination of the effects of CAR on glutamatergic and GABAergic activity via the analysis of PSCs induced in SubCD neurons. This study is an attempt to determine how the excitatory and inhibitory components of this area may be affected by cholinergic input, presumably from the PPN/LDT, to modulate arousal states.

METHODS

Pups aged 7–20 days from adult timed-pregnant Sprague-Dawley rats (280–350 g) were anesthetized with ketamine (70 mg/kg, I.M.) until tail pinch reflex was absent. This age range was selected because of the developmental decrease in REM sleep of the rat that occurs between 10 and 30 days.³³ This period of investigation enabled sampling from a baseline period (7–12 days), as well as the epoch of the greatest transitions between 12 and 20 days, as determined by our previous body of work on the PPN.^{34,35} Pups were decapitated, and the brain was rapidly removed and cooled in oxygenated sucrose-artificial cerebrospinal fluid (sucrose-aCSF). The sucrose-aCSF consisted of (in mM): 233.7 sucrose, 26 NaHCO₃, 8 MgCl₂, 0.5 CaCl₂, 20 glucose, 0.4 ascorbic acid, and 2 sodium pyruvate. Coronal sections (400 μm) containing the SubCD were cut, and slices were allowed to equilibrate in normal aCSF at room temperature for 1 hr. The aCSF was composed of (in mM): NaCl 117, KCl 4.7, MgSO₄ 1.2, CaCl₂ 2.5, NaH₂PO₄ 1.2, NaHCO₃ 24.9, and glucose 11.5. Slices were recorded at 30°C while superfused (1.5 mL/min) with oxygenated (95% O₂-5% CO₂) normal aCSF. Differential interference contrast optics was used to visualize neurons using an upright microscope (Nikon FN-1, Nikon, USA). All experimental protocols were approved by the Institutional Animal Care and Use Committee of the University of Arkansas for Medical Sciences and were in agreement with the National Institutes of Health guidelines for the care and use of laboratory animals.

Whole-cell recordings were performed using borosilicate glass capillaries pulled on a P-97 puller (Sutter Instrument Company, Novato, CA) and filled with a solution of (in mM): 124 K-gluconate, 10 HEPES, 10 phosphocreatine di tris, 0.2 EGTA, 4 Mg₂ATP, 0.3 Na₂GTP. In some experiments, Na₂GTP was replaced with the G-protein antagonist GDP-β-S (1 mM). For histological purposes, some recordings were conducted with 0.02% Lucifer yellow added to the intracellular solution, while 0.3% neurobiotin (Vector laboratories, Burlingame, CA) was used in the remaining recordings. Osmolarity was adjusted to ~270–290 mOsm and pH to 7.4. Holding potentials (HP) were set close to resting membrane potential at –50 mV. In these studies, we did not address electrical coupling, but in some experiments we recorded SubCD neurons (n = 6) with spikelets in the presence of QX-314 in the recording electrode. The spikelets observed in SubCD cells could in theory be from sodium-mediated dendritic spikes instead of electrically coupled neurons. The intracellular sodium channel antagonist QX-314 would have blocked all dendritic spikes, but the spikelets always remained. In some experiments, the voltage gated sodium channel blocker QX-314 (10 mM) and 1,2-Bis (2-amino-phenoxy) ethane-N,N,N',N'-tetraacetic acid tetrapotassium salt (10 mM BAPTA) and cesium methanesulfonate (124 mM) were used in place of K-gluconate to allow voltage clamp re-

cordings to be conducted at a HP between –10 and 0 mV to enhance inhibitory postsynaptic current (IPSC) detection. The pipette resistance was 5–10 MΩ. No series resistance compensation was performed in this study. The pipette series resistance may increase during an experiment because of an increase in pipette clogging or a slight drift of the cell surface away from the pipette. However, neurons with access resistance exceeding 20 MΩ were excluded from the analysis. All recordings were made using a MultiClamp 700B amplifier (Molecular Devices, Sunnyvale, CA). Analog signals were low-pass filtered at 2 kHz and digitized at 5 kHz using a Digidata-1322A and pClamp9 software (Molecular Devices, Sunnyvale, CA). Bath-applied drugs were administered to the slice via a peristaltic pump (Cole-Parmer, Vernon Hills, IL) and a 3-way valve system. Carbachol (CAR, 50 μM), tetrodotoxin citrate (TTX, 1 μM), 6-cyano-7-nitroquinoxaline-2,3-dione (CNQX, 10 μM), gabazine (GBZ, 10 μM), strychnine hydrochloride (STR, 10 μM), and (±)-2-amino-phosphopentanoic acid (APV, 10 μM), mecamylamine (MEC, 10 μM), atropine (ATR, 10 μM), pirenzepine (PRZ, 10 μM), methoctramine (MTO, 2 μM), barium chloride (BaCl₂, 1 mM), and physostigmine (PHY, 10 μM) were all purchased from Sigma (St. Louis, MO). CAR was applied at 50 μM to ensure a saturating effect of CAR in each application. Consequently, slightly higher concentrations of the competitive antagonists PRZ and MTO were used to block this effect. While the muscarinic subtype binding specificity of PRZ and MTO are not ideal, studies have demonstrated that these doses are specific to the M1 and M2 receptors, respectively, in slices of neural tissue.³⁶ While previous studies have established the presence of nicotinic receptors in the SubCD, only minimal labeling of α7 nicotinic receptors has been found in this region.³⁷⁻³⁹ Mecamylamine has been widely used in the past and shown to be a potent antagonist to the nicotinic receptors.⁴⁰⁻⁴¹ The input resistance was calculated by measuring the initial current produced by a hyperpolarizing voltage step from –50 to –100 mV in voltage clamp mode. Relative hyperpolarization-activated inward current (I_h) ratios were determined in voltage clamp by calculating the difference between the current measured at the end of a 0.5-sec hyperpolarizing step (–50 to –100 mV) and that measured at the initiation of this step. The calculated difference was then divided by the current produced at the initiation of the hyperpolarizing step.^{42,43} This protocol produced the amount of I_h current normalized to the input conductance of each cell, which was assumed to be generally proportional to the size of the cell. All recorded neurons were located ventral to the locus coeruleus (LC). Suspected LC neurons were excluded from analysis based on physiological characteristics, such as spontaneous pacemaker-like (1-2 Hz) firing pattern and a large outward I_A current.^{44,45} The liquid-junction potential was ~9 mV for pipettes filled with K-gluconate intracellular solution, and the reported voltages were not corrected for this value (except when indicated in experiments where we calculated the reversal potential of the response to cholinergic receptor agonists).

Electrical Stimulation

Stimulation of the SubCD was performed using bipolar tungsten electrodes (FHC, Bowdoin, ME). The stimulating electrodes (200 KΩ) were placed 50–200 μm from the recorded

neurons. Paired-pulse stimuli were delivered at 30-ms intervals every 5 sec. Pulse duration was 0.1 msec, and voltage was adjusted from 2–30 V. Similar stimulation protocols have been used in several previous studies to evoke a consistent response with low failure rate ($1.5\text{--}1.7 \times$ threshold).^{44,46} Pulses were delivered with an S-88 stimulator connected to an SIU5 stimulus isolation unit (Grass Instruments, Warwick, RI).

Data Analysis

Off-line analyses were performed using Clampfit software (Molecular Devices, Sunnyvale, CA). The quantification of PSCs was performed using the program Mini Analysis (Synaptosoft, Decatur, GA). CAR was observed to increase baseline noise in 10% to 20% of SubCD neurons; however, no trend was evident during CAR that was different from control conditions. Consequently, detection thresholds were set to be a minimum of 5 times the root mean square value measured during peak CAR effect. This ensured that nonspecific currents activated by CAR were not counted in these analyses. The PSC parameters were then imported to Origin 7.0 (Microcal Software, Northampton, MA). Analysis conditions consisted of 50-s windows prior to CAR application, during peak CAR effect, and after CAR had washed. For comparison of data between different groups, means were collected for each condition in each cell, and paired *t*-tests were used to analyze differences across conditions. *F* values and degrees of freedom were reported for all linear regression ANOVAs. Differences were considered significant at values of $P \leq 0.05$. All results are presented as mean \pm SEM.

RESULTS

Anatomical Localization of SubCD Neurons

All experiments were conducted in rat pup brain slices using anatomical coordinates corresponding to adult brain coronal sections located between -9.68 and -9.16 mm posterior to bregma.⁴⁷ The locations of recorded cells were determined using histological verification of neurobiotin or Lucifer yellow injected cells. All neurons were located in a region ~ 500 μm in diameter anterior to the 7th nerve in the region of the rat brainstem termed dorsal SubCD. Although tyrosine hydroxylase immunocytochemistry was not performed, most recordings were well ventral to the locus coeruleus and scattered tyrosine hydroxylase-positive neurons. Some sections were processed for nitric oxide synthase (NOS) immunocytochemistry, which selectively labels cholinergic mesopontine neurons; no NOS-positive cells were found within the region sampled. We did not attempt to identify different morphological or neurotransmitter types in this population, but suspect they represent a mixture of glutamatergic and GABAergic neurons. Figure 1A shows a representative region of the SubCD in which recordings were performed. A bright field photomicrograph superimposed on a fluorescent image of 2 recorded SubCD neurons (filled with Lucifer yellow) are indicated within the marked boundary. Figure 1B is a magnified confocal image of the same 2 neurons. The coronal section corresponding to Figure 1A can be seen within the marked boundary of the -9.3 mm

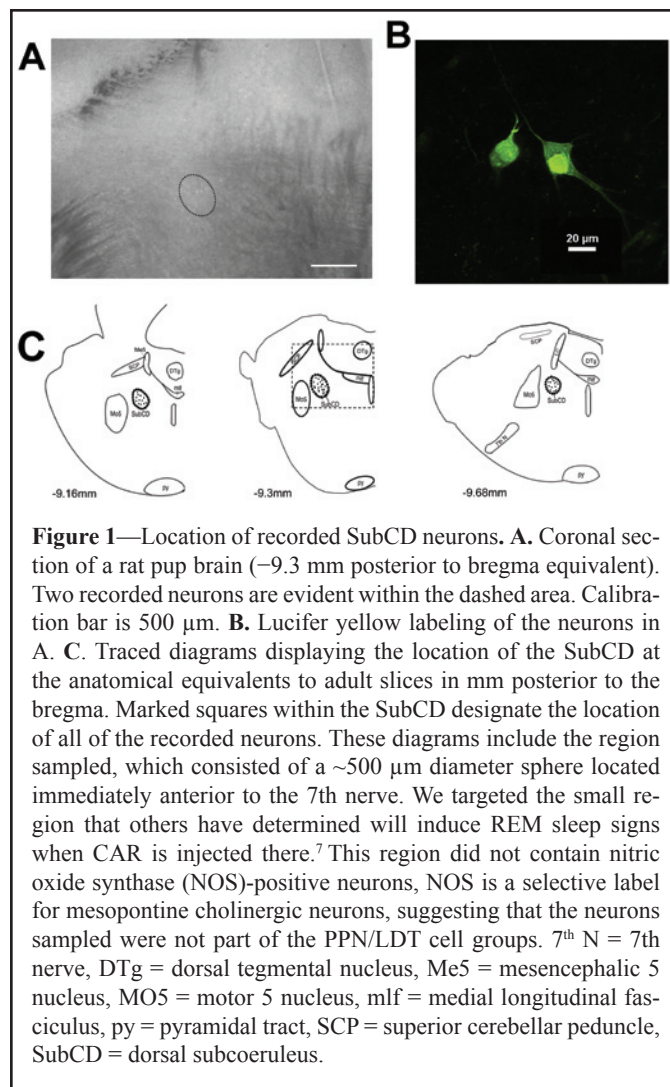
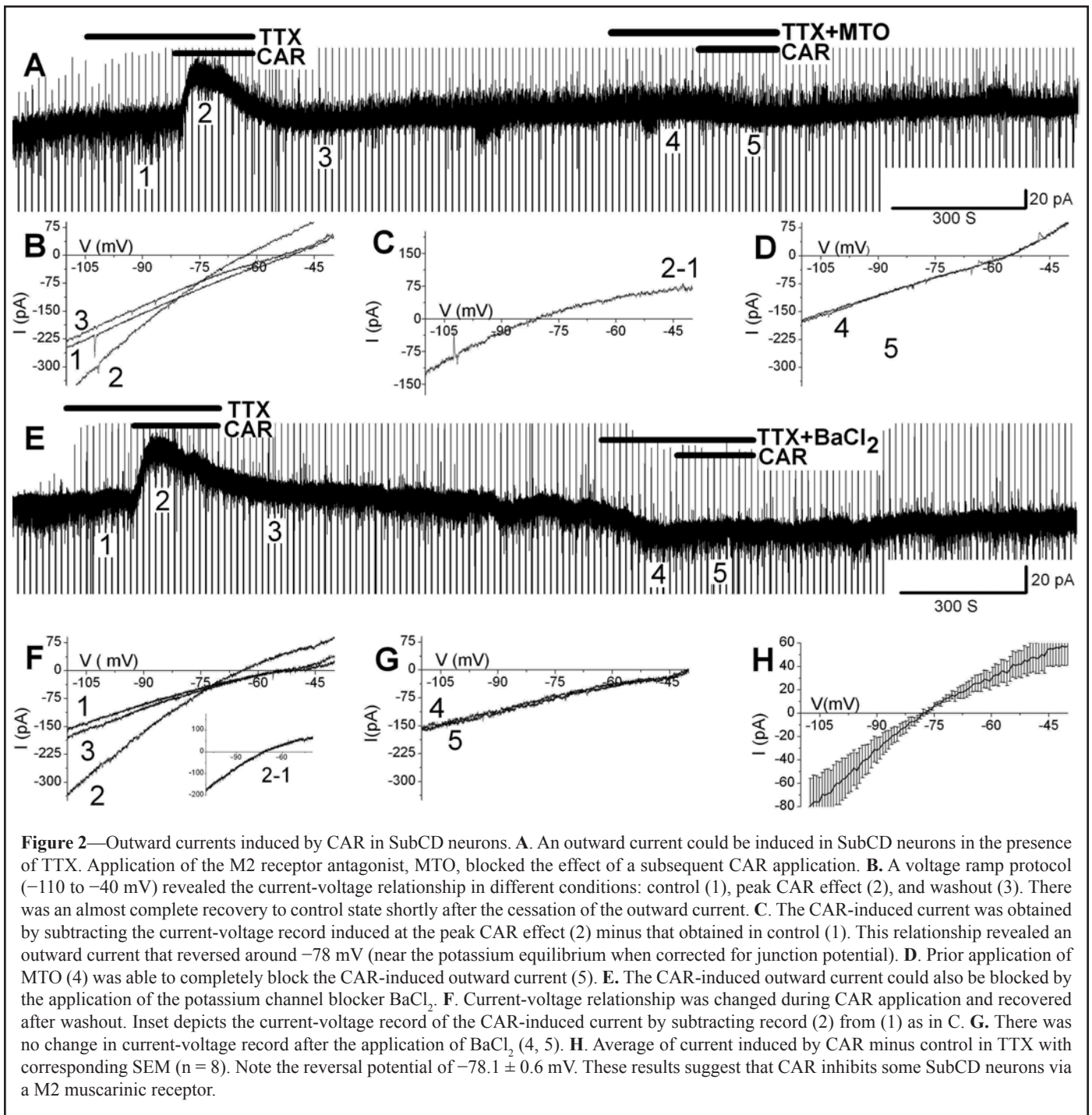


Figure 1—Location of recorded SubCD neurons. **A.** Coronal section of a rat pup brain (-9.3 mm posterior to bregma equivalent). Two recorded neurons are evident within the dashed area. Calibration bar is 500 μm . **B.** Lucifer yellow labeling of the neurons in **A.** **C.** Traced diagrams displaying the location of the SubCD at the anatomical equivalents to adult slices in mm posterior to the bregma. Marked squares within the SubCD designate the location of all of the recorded neurons. These diagrams include the region sampled, which consisted of a ~ 500 μm diameter sphere located immediately anterior to the 7th nerve. We targeted the small region that others have determined will induce REM sleep signs when CAR is injected there.⁷ This region did not contain nitric oxide synthase (NOS)-positive neurons, NOS is a selective label for mesopontine cholinergic neurons, suggesting that the neurons sampled were not part of the PPN/LDT cell groups. 7th N = 7th nerve, DTg = dorsal tegmental nucleus, Me5 = mesencephalic 5 nucleus, MO5 = motor 5 nucleus, mlf = medial longitudinal fasciculus, py = pyramidal tract, SCP = superior cerebellar peduncle, SubCD = dorsal subcoeruleus.

equivalent section. Each traced section in Figure 1C displays the anatomically corresponding adult distance posterior to the bregma.

Postsynaptic Effects of CAR

Whole-cell voltage clamp recordings (HP = -50 mV) of SubCD neurons ($n = 108$) revealed that bath application of CAR produced similar results as in previous studies.^{28,30,31} In the presence of TTX, CAR induced an outward current (44.3 ± 9.7 pA; $n = 46$) in 43% of SubCD neurons and an inward current (-40.5 ± 5.1 pA; $n = 54$) in 50% of the neurons, whereas there was no discernible effect in the remaining 7% ($n = 8$). There was no significant change in the response of SubCD cells when CAR was applied in the absence of TTX ($n = 8$ outward cells, $n = 18$ inward cells; $P > 0.05$). Repeated applications of CAR for 3 min followed by washing for 10 min revealed that subsequent CAR responses were decreased in amplitude by $19\% \pm 4\%$ in up to 3 applications ($n = 9$). This decrease was present in cells displaying both inward and outward currents. These tests showed that, while SubCD neurons did show some habituation, CAR induced a large reproducible effect in these neurons in a second and even third application. Voltage ramps (HP stepped to -110 mV for 0.5 sec then ramped to -40 mV over 1 sec), and antago-



nists were used to determine the reversal potentials and the possible receptors mediating the effects of CAR in this nucleus.

Outward Currents

CAR induced an outward current in the presence of TTX in 43% of SubCD neurons, and examples are provided in Figure 2. Application of the M2 antagonist, methoctramine (MTO), blocked the effect of subsequent CAR applications in every cell tested (Figure 2A; n = 6). The current-voltage relationship was analyzed in different conditions: control (1, $R_{in} = 364 \pm 107 \text{ M}\Omega$), peak CAR effect (2, $R_{in} = 231 \pm 72 \text{ M}\Omega$), and washout of CAR (3, $R_{in} = 319 \pm 91 \text{ M}\Omega$) ($P < 0.05$; n = 6; Fig-

ure 2B). After CAR washout, there was an almost complete recovery to the control state shortly after the cessation of the outward current (note the similarity of ramp 1 and ramp 3 in Figure 2B). Subtracting the current ramp induced at the peak CAR effect (2) from the control ramp (1) revealed the current induced by CAR (Figure 2C). This subtraction revealed that CAR generated an outward current that reversed around –78 mV, which was near the potassium equilibrium potential (calculated to be –85 mV, and the corrected liquid junction potential being around –76 mV) when corrected for the junction potential, in this neuron. After 10 min of washing, a second application of CAR in the presence of the M2 muscarinic receptor antagonist, MTO, produced no changes in holding cur-

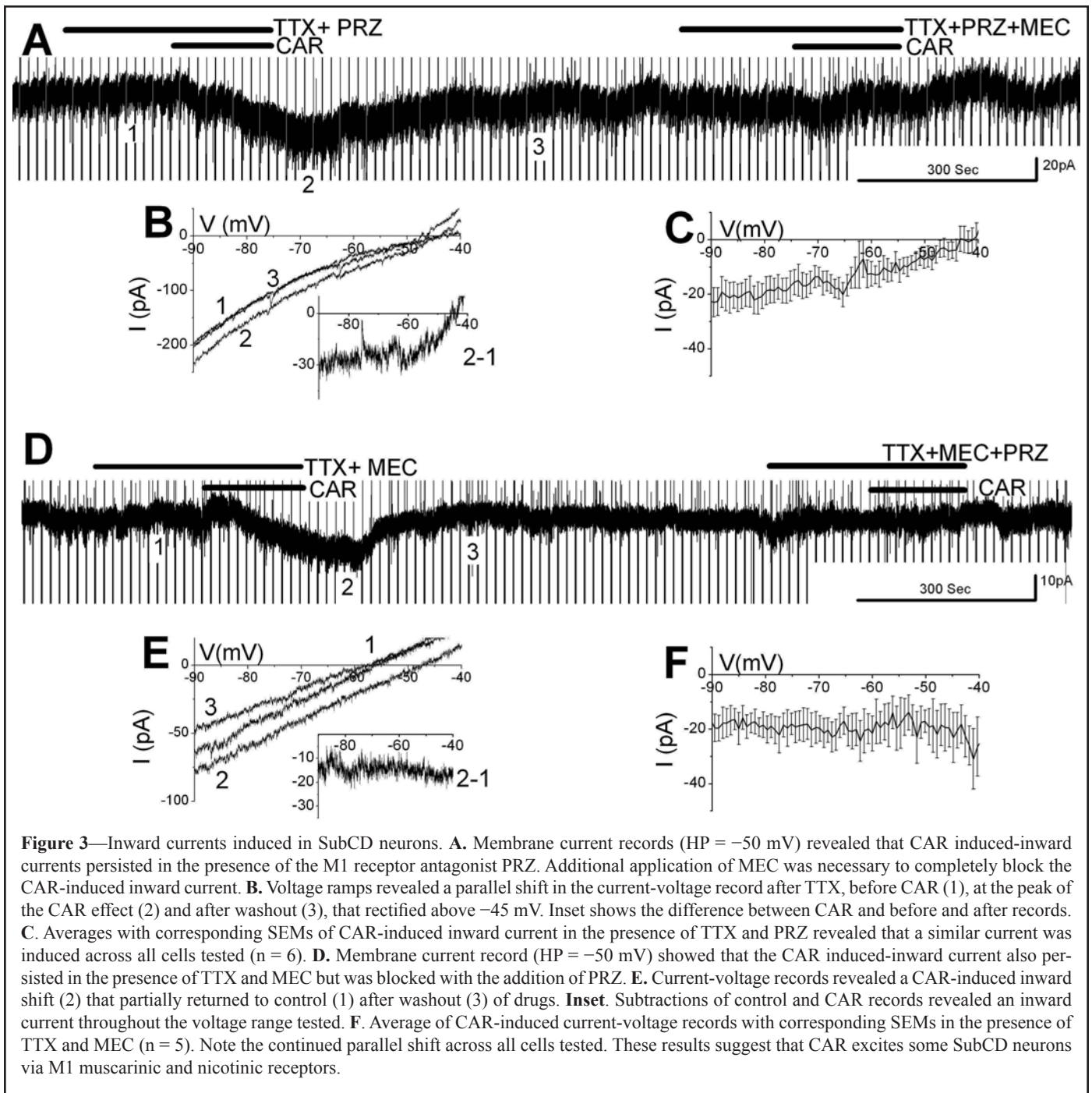


Figure 3—Inward currents induced in SubCD neurons. **A.** Membrane current records (HP = -50 mV) revealed that CAR induced inward currents persisted in the presence of the M1 receptor antagonist PRZ. Additional application of MEC was necessary to completely block the CAR-induced inward current. **B.** Voltage ramps revealed a parallel shift in the current-voltage record after TTX, before CAR (1), at the peak of the CAR effect (2) and after washout (3), that rectified above -45 mV. Inset shows the difference between CAR and before and after records. **C.** Averages with corresponding SEMs of CAR-induced inward current in the presence of TTX and PRZ revealed that a similar current was induced across all cells tested ($n = 6$). **D.** Membrane current record (HP = -50 mV) showed that the CAR induced inward current also persisted in the presence of TTX and MEC but was blocked with the addition of PRZ. **E.** Current-voltage records revealed a CAR-induced inward shift (2) that partially returned to control (1) after washout (3) of drugs. **Inset.** Subtractions of control and CAR records revealed an inward current throughout the voltage range tested. **F.** Average of CAR-induced current-voltage records with corresponding SEMs in the presence of TTX and MEC ($n = 5$). Note the continued parallel shift across all cells tested. These results suggest that CAR excites some SubCD neurons via M1 muscarinic and nicotinic receptors.

rent or Rin (holding current -16 ± 9 pA before MTO vs -13 ± 8 pA after MTO application vs -16 ± 9 after MTO+CAR; Rin 330 ± 100 vs 316 ± 80 vs 321 ± 95 , $P > 0.05$ for both current and Rin, $n = 6$; Figure 2D).

In separate experiments, BaCl_2 , a blocker of the inwardly rectifying potassium current, was also effective in blocking the CAR-induced outward current in every cell tested (Figure 2E; $n = 4$). In control conditions, voltage ramps (Figure 2F) revealed similar decreases in input resistance by CAR (Rin decreased from 292 ± 64 M Ω to 167 ± 35 M Ω in these cells, similar to the decrease previously reported.^{28,48} The CAR-induced current again reversed near -78 mV (Figure 2F inset). The subsequent addition of BaCl_2 blocked the effects of further CAR application (Figure 2G).

Averaging the current-voltage recordings induced by CAR in these “outward” cells revealed an average reversal potential of -78.1 ± 0.6 mV which, when corrected for the liquid-junction potential (Figure 2H; $n = 8$). These results indicate that the CAR-induced outward current of SubCD neurons may be mediated by activation of M2 receptors and the subsequent opening of potassium channels.

Inward Currents

In the presence of TTX, cells that responded to CAR with an inward current exhibited a wide range of reversal potentials of these currents and a decrease in input resistance (from $239 \pm$

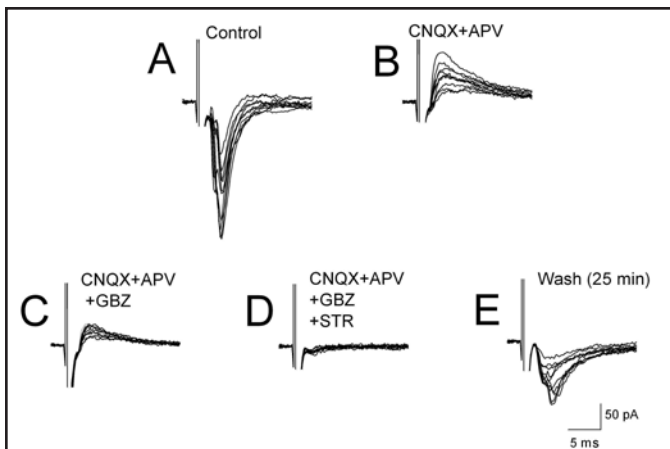


Figure 4—Pharmacological characterization of evoked PSCs in the SubCD. **A.** Superimposed EPSCs of variable amplitude were elicited using constant intensity stimulation at intervals of 5 sec. **B.** Underlying evoked IPSCs were revealed during blockade of fast synaptic transmission with CNQX and APV. **C.** Evoked IPSCs were reduced in amplitude in the presence of GBZ. **D.** The application of both GBZ and STR was necessary to completely block evoked IPSCs. **E.** The evoked EPSCs partially recovered after 25 min of drug washout. Ten superimposed records of evoked PSCs are shown in each panel. The stimulus artifact was truncated for clarity. These results established that electrical stimulation of the SubCD induced both excitation and inhibition in SubCD neurons consistent with the presence of glutamatergic and GABAergic inputs to these cells. The CAR effects on these evoked responses could be mimicked by endogenously released acetylcholine (see Figures 5-7).

26 M Ω before CAR to 169 \pm 13 M Ω after CAR, $P < 0.05$, $n = 9$). These results suggest that a variety of ion channels may be involved in the CAR-induced inward current. Experiments revealed that the CAR-induced inward currents may involve both nicotinic and M1 muscarinic receptors since application of antagonists of both types of receptors was necessary to completely block the CAR-induced current (Figure 3A and 3D; $n = 9$).

Application of CAR in the presence of TTX and pirenzepine (PRZ), an M1 receptor antagonist, continued to induce an inward current (Figure 3A). Current-voltage relationship analysis of these experiments revealed that CAR (Figure 3B, record 2) decreased the input resistance (from 252 \pm 30 M Ω to 165 \pm 11 M Ω ; $n = 6$) and produced a current with a relatively depolarized reversal potential. Subtracting the current-voltage record in control from that obtained during CAR revealed that the current induced by CAR in one cell rectified and reversed near -47 mV (Figure 3B, inset). Averaging CAR-induced current-voltage records in the presence of TTX and PRZ across cells revealed the presence of a rectifying current that reversed at -43 \pm 1.9 mV (Figure 3C; $n = 6$). This current was then completely blocked with the addition of the nicotinic antagonist mecamylamine (MEC) (Figure 3A). The addition of MEC had no significant effect on holding current (-24 \pm 10 pA before vs -21 \pm 9 pA after MEC). These experiments suggest that a nicotinic inward current may be activated by CAR in at least some SubCD neurons.

CAR also induced an inward current in the presence of TTX and the nicotinic antagonist mecamylamine (MEC) (Figure 3D; $n = 5$). Voltage ramp protocols in control, and in the presence of CAR revealed a parallel shift in the current-voltage recordings

indicating that CAR produced an inward current that exhibited little rectification (Figure 3E; $n = 5$). This parallel shift in the current-voltage record can be observed when the control period (record 1) was subtracted from that obtained during CAR application (record 2; see inset of Figure 3E). A comparison of Figure 3C and 3F reveals that the CAR induced inward currents exhibited in the presence of either PRZ or MEC had identifiably different rectifying characteristics. After the addition of both PRZ and MEC, some experiments even suggested the presence of a small CAR-induced outward current ($n = 4$, Figure 3A), suggestive of the presence of M2 receptors. These results may indicate that the CAR-induced inward current observed in the SubCD was probably mediated by currents via both M1 and nicotinic receptors. Moreover, M2 receptors may be co-localized with M1 and nicotinic receptors on some SubCD neurons that more typically exhibit an inward current in response to CAR.

Developmental Changes in Intrinsic Properties and CAR Responses

SubCD neurons were recorded from 7-20 day old rats in an attempt to examine whether there were any developmental changes in their intrinsic properties or responses to CAR. The input resistance decreased over this developmental period from 515 \pm 51 M Ω ($n = 31$) in 7- to 8-day-old SubCD neurons to 316 \pm 61 M Ω ($n = 11$) in 19- to 20-day-old SubCD neurons (ANOVA; $df = 165$; $F = 5.79$; $r = -0.184$; $P < 0.05$; $n = 167$). The mean resting membrane potential also exhibited a decreasing trend from -50.8 \pm 3.1 mV (days 7-8; $n = 10$) to -54.6 \pm 3.0 mV (days 19-20; $n = 13$) throughout this period (ANOVA; $df = 79$; $F = 4.33$; $r = -0.228$; $P < 0.05$; $n = 81$). Furthermore, analysis of the amplitude of the hyperpolarization-activated inward current (I_h) revealed a nonsignificant decreasing trend across development. The mean I_h ratio (see Methods) ranged from 0.20 \pm 0.03 (days 7-8; $n = 28$) to 0.18 \pm 0.07 (days 19-20; $n = 10$) (ANOVA; $df = 233$; $F = 3.35$; $r = -0.119$; $P = 0.068$; $n = 235$). Note, however, that pharmacological identification of this current using ZD-7288 was not carried out.

Conversely, the peak direct current produced by CAR (i.e. in the presence of TTX) was not correlated with age (ANOVA; $df = 106$; $F = 0.023$; $r = -0.015$; $P > 0.05$; $n = 108$). While the decrease in both input resistance and resting potential of these neurons may indicate a general decrease in excitability over this period, the mechanisms underlying the effects of CAR on SubCD neurons seem to be largely in place by the end of the first postnatal week in rat pups. Finally, there were no detectable correlations between specific CAR effects and input resistance, resting membrane potential, or relative I_h .

CAR Effects on Evoked EPSCs

A bipolar stimulating electrode placed 50–200 μ m from whole-cell patched SubCD neurons ($n = 17$) was used to evoke PSCs (see example in Figure 4A). Evoked EPSCs could always be blocked with the combined application of the AMPA receptor antagonist CNQX and the NMDA antagonist APV ($n = 17$; Figure 4B). The application of the GABA_A receptor antagonist, GBZ, (Figure 4C) reduced the evoked IPSCs to 35% \pm 10.5% of the control amplitude, whereas additional application

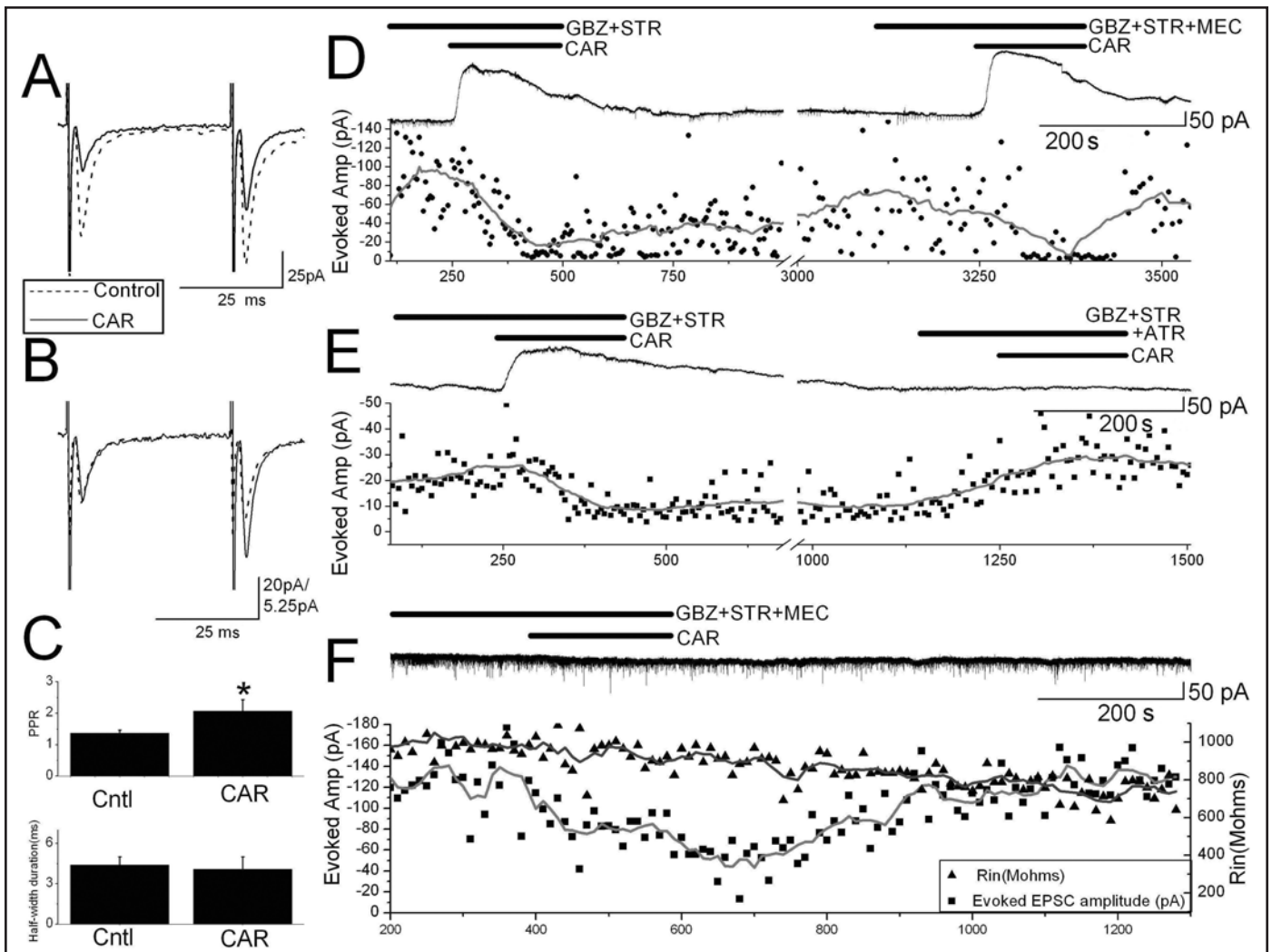


Figure 5—SubCD responses following electrical stimulation. **A.** Average of 5 evoked EPSCs in GBZ and STR control (dashed) and after addition of CAR (solid). Note records were shifted to the same baseline to allow amplitude comparison. **B.** The PPF ratio increased during application of CAR. CAR preferentially decreased the first evoked EPSC, suggesting a presynaptic effect. The first CAR-evoked EPSC was scaled to match the first control EPSC. Vertical calibration is 20 pA and 5.25 pA for the control and CAR records, respectively. **C.** The PPR was significantly increased ($*P < 0.05$) from control by the application of CAR in all cells tested ($n = 22$). This increase in the PPR implies that CAR preferentially decreased the amplitude of the first evoked EPSC. These data suggest that CAR may modulate the probability of transmitter release by activating cholinergic receptors on presynaptic glutamatergic terminals. The half-width duration did not change significantly between groups ($n = 22$). **D.** In the presence of GBZ and STR, CAR induced an outward current (top record) in a cell recorded in voltage clamp at a HP = -50 mV. Lower scatter plots show the amplitude of EPSCs evoked by electrical stimulation every 5 sec and a 25-point smoothed average of the EPSC amplitude. The effects of CAR on the membrane current and the evoked EPSCs persisted in the presence of the nicotinic receptor antagonist, MEC. **E.** In another SubCD cell, CAR induced an outward current (top record) and decreased the evoked EPSCs (bottom plot), and these effects were blocked by ATR ($10 \mu\text{M}$). **F.** In the presence of GBZ, STR, and MEC extracellularly, and GDP- β -S in the intracellular solution, CAR decreased the evoked EPSC amplitude without changing the input resistance or holding current.

of the glycine receptor antagonist, STR, completely blocked the remaining evoked IPSCs (Figure 4D; $n = 4$). This suggests that the evoked IPSCs within this area were mediated by both GABA_A and glycine receptors. All PSCs returned with washing (Figure 4E).

In order to determine whether cholinergic receptors modulate neurotransmitter release, the effects of CAR on pharmacologically isolated excitatory and inhibitory PSCs were investigated. Both GBZ and STR were bath-applied for 3 min prior to and throughout the application of CAR in order to isolate evoked EPSCs. In these conditions, CAR decreased the amplitude of evoked EPSCs in 31 of 34 SubCD neurons from 78.3 ± 9.4 pA

to 36.6 ± 6.0 pA ($t = -8.18$; $df = 33$, $P < 0.001$; $n = 34$; Figure 5A). In 2 of 34 neurons, there was no significant effect (< 3 pA change), and one of 34 neurons showed an increase in evoked EPSCs. There was no apparent correlation between the effects of CAR on membrane current (inward vs. outward current) and the change in amplitude of evoked EPSCs. The cholinesterase inhibitor, physostigmine (PHY), was also used to test whether the effects of CAR on the evoked EPSCs could be reproduced by endogenously-released acetylcholine. Application of PHY in the presence of GBZ and STR decreased evoked EPSCs in all neurons tested from 119.4 ± 33.6 pA to 83.9 ± 28.3 pA ($t = -3.70$; $df = 5$; $P < 0.05$; $n = 6$). This indicated that the CAR

effects on evoked EPSCs could be mimicked by endogenously released acetylcholine.

Paired-pulse stimulation revealed that SubCD neurons exhibited paired-pulse facilitation (PPF), which is defined as an increase in the amplitude of the EPSC response to the second of a pair of closely spaced stimuli (Figure 5B). It is generally thought that PPF results from residual increases in calcium concentration in the presynaptic terminal after an initial stimulus.^{49,50} Thus, a change in the paired-pulse ratio (PPR, amplitude of the second evoked EPSC divided by the first one) suggests modulation of presynaptic terminals because a pure postsynaptic effect is expected to be translated into identical changes in the responses to both pulses. The PPR was significantly increased from control (PPR 1.4 ± 0.1) by application of CAR (PPR 2.1 ± 0.4 ; $t = -2.48$; $df = 21$; $P < 0.05$; $n = 22$; Figure 5C). This increase in the PPR implies that CAR preferentially decreased the amplitude of the first evoked EPSC. These data indirectly suggest that CAR may modulate the probability of transmitter release by activating cholinergic receptors on presynaptic glutamatergic terminals.

Furthermore, the evoked EPSC half-width duration was not significantly changed from control (4.41 ± 0.59 msec) following CAR application (4.10 ± 0.91 msec; $t = 0.37$; $df = 21$; $P > 0.05$; $n = 22$; Figure 5C). This suggests that the kinetic properties of the postsynaptic ionotropic glutamate receptors were probably not altered by activation of cholinergic receptors. The time to peak and decay of the EPSCs was not analyzed in detail since no obvious differences were observed in control vs CAR conditions in any early experiments.

Additional experiments were performed to determine the type of cholinergic receptors responsible for the CAR-induced decrease in evoked EPSCs. In the presence of GBZ and STR, CAR decreased the amplitude of evoked EPSCs by 35% (from 80.9 ± 18.0 pA to 52.3 ± 18.6 pA; t value = -3.50 ; $df = 6$; $P < 0.05$; $n = 7$). A second application of CAR in the presence of GBZ, STR, and MEC, the nicotinic antagonist, also decreased the amplitude of the evoked EPSCs by an average of 43% from 71.6 ± 17.6 pA to 41.0 ± 11.5 pA ($t = -3.34$; $df = 6$; $P < 0.05$; $n = 7$; Figure 5D). These results suggest that the cholinergic receptors involved in the decrease in evoked EPSCs were probably in large part non-nicotinic. Additionally, the previous experiments established that the CAR-induced decrease in evoked EPSCs was reproducible at least twice with little habituation.

In contrast to MEC, the nonspecific muscarinic antagonist, atropine (ATR), prevented the decrease in the amplitude of evoked EPSCs in response to a second application of CAR in all cells tested (Figure 5E). The M2 specific antagonist, MTO, also prevented the decrease in the amplitude of evoked EPSCs in response to a second application of CAR in 5 of 8 cells. The remaining 3 cells continued to show a CAR-induced decrease in evoked EPSCs in the presence of MTO. This suggests that, in the SubCD, the inhibitory cholinergic effects on evoked EPSCs were predominantly mediated by M2 receptors. However, it is possible that some SubCD neurons may also possess other muscarinic receptors that can contribute to the inhibition of evoked EPSCs.

Further control experiments were conducted in order to isolate the CAR-induced decrease in evoked EPSCs from CAR-

induced changes in input resistance. These protocols served to ensure that the observed CAR-induced decreases in evoked EPSCs were *not* due to postsynaptic alterations in membrane properties often known as shunting. Previous studies have shown that the effects of CAR can be blocked via the use of the intracellular g protein antagonist GDP- β -S.^{51,52} Our experiments used a modified intracellular solution by replacing GTP with the G-protein antagonist GDP- β -S (1 mM). The input resistance and the amplitude of evoked EPSCs were simultaneously measured during the exposure of a brain slice to GBZ, STR, and MEC for 3 min followed by CAR application. The addition of extracellular MEC and the intracellular GDP- β -S were successful in blocking the direct postsynaptic effects of CAR on all of the recorded neurons as demonstrated by an absence of changes in either holding current or input resistance (control: 680 ± 143 M Ω ; 42.8 ± 7.3 pA; CAR = 647 ± 118 M Ω , 44.2 ± 7.8 pA; $t = 1.05$; $df = 5$; $P = 0.21$ for holding current; $P = 0.4$ for R_{in} ; $n = 6$; Figure 5F). In contrast, the evoked EPSCs were still reduced by CAR from 103.1 ± 31.9 pA to 57.3 ± 23.9 pA ($t = -4.53$; $df = 5$; $P < 0.01$; $n = 6$; Figure 5F). There was also a nonsignificant trend towards of increasing PPR in these conditions (Control PPR = 1.2 ± 0.2 ; CAR PPR = 2.1 ± 0.4 ; $P > 0.05$; $n = 6$). This demonstrated that the CAR-induced inhibition evoked EPSCs was not solely a result of postsynaptic modulation of the recorded cell.

At the end of each preceding experiment, the types of glutamatergic receptors mediating the evoked EPSCs were determined first via application of CNQX, then by additional application of APV if the EPSCs persisted. CNQX alone was able to block the evoked EPSCs in most cells ($n = 15$ of 17). However, in 2 of 17 cells, the addition of both APV and CNQX was required to completely block the evoked response. This indicated that, in our experimental conditions (HP = -50 mV), the evoked EPSCs were mediated mainly via AMPA/kainate receptors in the SubCD, while NMDA receptors may also have contributed to the excitatory response in some cells.

CAR Effects on Evoked IPSCs

We first investigated the effects of CAR on evoked IPSCs using a standard potassium gluconate intracellular solution in the presence of CNQX and APV to block fast synaptic glutamatergic inputs. In these conditions, we were able to evoke detectable outward IPSCs (14.6 ± 6.6 pA control) at HP = -50 mV, but 75% (3 of 4 cells) of experiments revealed inconclusive changes in response to CAR application (19 ± 8.6 pA). This protocol was then modified in order to maximize the detection of IPSCs by using an intracellular solution containing QX-314, cesium methane sulfate to block sodium and potassium channels, respectively, and BAPTA to buffer intracellular calcium concentration. In these conditions, we were able to record relatively larger outward evoked IPSCs (49.9 ± 18.4 pA; control) at a HP of 0 mV. Nevertheless, CAR application induced an increase in evoked IPSCs in only 1 of 13 neurons while the remaining neurons showed no changes in evoked IPSCs in response to CAR application (51.9 ± 14.3 pA). Taken together, these results suggest that CAR probably depressed evoked SubCD glutamatergic transmission without affecting evoked inhibitory neurotransmitter release.

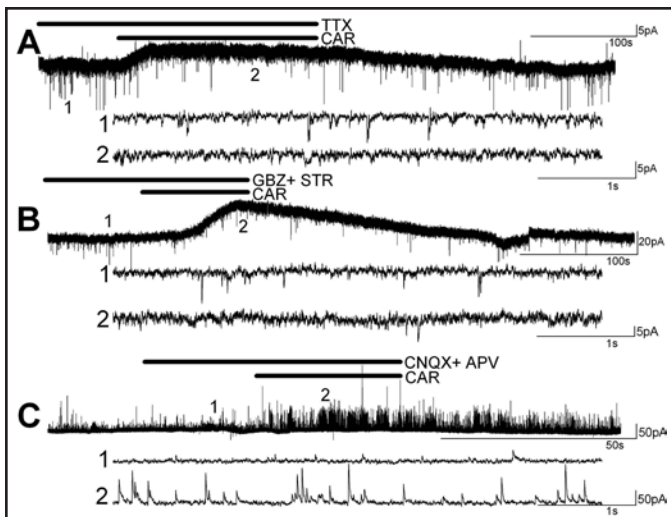


Figure 6—Modulation of spontaneous PSCs by CAR. **A.** Membrane current record (HP = -50 mV) of a SubCD neuron showing the effects of CAR on miniature EPSCs in the presence of TTX. Note the outward current and the decrease in miniature EPSC frequency during CAR application. **B.** Membrane current record (HP = -50 mV) of a SubCD neuron in the presence of GBZ and STR. CAR decreased the frequency of spontaneous EPSCs and induced an outward current in this cell. **C.** Voltage clamp recording (HP = 0 mV with QX-314, cesium, and BAPTA in the intracellular solution) showing the effect of CAR on spontaneous IPSCs in the presence of blockers of fast excitatory synaptic transmission (CNQX and APV). CAR produced a large increase in the frequency of IPSCs in these conditions.

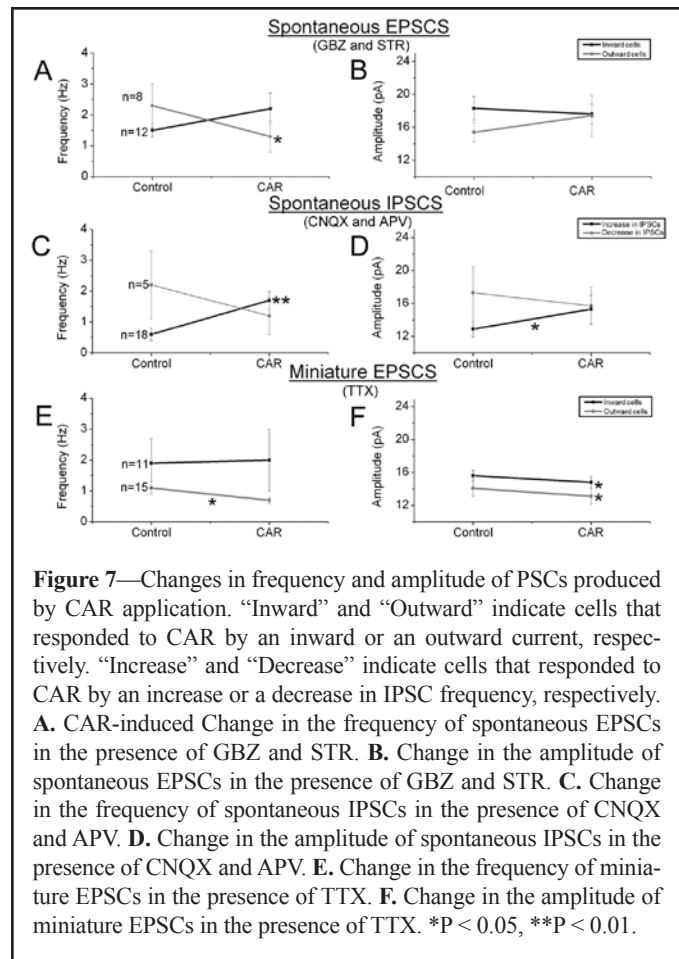


Figure 7—Changes in frequency and amplitude of PSCs produced by CAR application. “Inward” and “Outward” indicate cells that responded to CAR by an inward or an outward current, respectively. “Increase” and “Decrease” indicate cells that responded to CAR by an increase or a decrease in IPSC frequency, respectively. **A.** CAR-induced Change in the frequency of spontaneous EPSCs in the presence of GBZ and STR. **B.** Change in the amplitude of spontaneous EPSCs in the presence of GBZ and STR. **C.** Change in the frequency of spontaneous IPSCs in the presence of CNQX and APV. **D.** Change in the amplitude of spontaneous IPSCs in the presence of CNQX and APV. **E.** Change in the frequency of miniature EPSCs in the presence of TTX. **F.** Change in the amplitude of miniature EPSCs in the presence of TTX. * $P < 0.05$, ** $P < 0.01$.

CAR Effects on Spontaneous PSCs

The spontaneous postsynaptic currents (PSCs) recorded in SubCD cells typically correspond to the sum of action potential-dependent and action potential-independent PSCs. This was demonstrated with the application of TTX to SubCD neurons revealing a significant decrease in PSC frequency from 3.0 ± 0.91 Hz to 2.54 ± 0.87 Hz ($t = 2.5$; $df = 6$; $P < 0.05$; $n = 7$) but not amplitude (Control = 12.2 ± 1.02 pA; TTX = 11.9 ± 0.83 pA; $t = 0.53$; $df = 6$; $P > 0.05$; $n = 7$). These data suggest that at least a portion of the spontaneous PSCs were action potential-dependent.

The effects of CAR on spontaneous PSCs were initially analyzed by quantifying the frequency of PSCs before and during CAR application without any antagonists. EPSCs and IPSCs were recorded at a HP of -50 mV as inward and outward currents, respectively. During CAR application only, 55% of SubCD neurons showed a decrease in spontaneous EPSC frequency from 3.3 ± 1.2 Hz to 2.0 ± 0.9 Hz ($t = 2.55$; $df = 11$; $P < 0.05$; $n = 12$ of 22). In contrast, 27% of SubCD neurons showed an increase in spontaneous IPSC frequency from 0.85 ± 0.4 Hz to 4.2 ± 1.4 Hz ($t = -3.19$; $df = 5$; $P < 0.05$; $n = 6$ of 22). The remaining 18% of neurons showed an increase in EPSCs from 5.6 ± 2.5 Hz to 9.5 ± 3.0 Hz ($t = -3.81$; $df = 3$; $P < 0.05$; $n = 4$). CAR produced no significant changes in the above PSC amplitudes. Thus, in the majority of SubCD cells, CAR application apparently either increased spontaneous IPSCs or decreased spontaneous EPSCs ($n = 18$ of 22). These data suggest that CAR may predominantly enhance

inhibitory transmission and reduce excitatory transmission in the SubCD.

In order to more specifically examine whether CAR modulated spontaneous neurotransmitter release (Figure 6A), we analyzed the effects of CAR on spontaneous EPSCs in the presence of GBZ and STR (Figure 6B). In these conditions, the EPSC frequency was not significantly altered in cells exhibiting an inward current to CAR (Control = 1.5 ± 0.2 Hz; CAR = 2.2 ± 0.5 Hz; $t = -1.87$; $df = 10$; $P > 0.05$; $n = 11$; Figure 7A). However, in 7 of 8 cells exhibiting an outward current to CAR, the EPSC frequency decreased from 2.3 ± 0.7 Hz to 1.3 ± 0.5 Hz ($t = 2.48$; $df = 7$; $P < 0.05$; $n = 8$; Figure 6B, 7A). In contrast, the EPSC amplitude did not significantly change in any of the above conditions ($t = 1.34$, $P > 0.05$; $t = -1.29$, $P > 0.05$ respectively; Figure 7B).

To enhance the detection of spontaneous IPSCs, we recorded SubCD neurons in the presence of CNQX and APV at HP = 0 mV using an intracellular solution containing QX-314, cesium and BAPTA. CAR increased IPSC frequency from 0.6 ± 0.2 Hz to 1.7 ± 0.3 Hz ($t = -3.87$; $df = 17$; $P < 0.01$) in 18 of 23 neurons (Figure 6C, 7C). There was also a significant increase in spontaneous IPSC amplitude by CAR (Control = 12.9 ± 1.0 pA; CAR = 15.3 ± 1.7 pA; $t = -2.38$; $df = 17$; $P < 0.05$; $n = 18$; Figure 7D). In 5 neurons, there was a nonsignificant decrease in IPSC frequency and amplitude (control: 2.2 ± 1.1 Hz, 17.3 ± 3.2 pA; CAR: 1.2 ± 0.6 Hz, 15.7 ± 2.3 pA) (frequency $t = 1.92$; $df = 4$; $P > 0.05$; amplitude $t = 1.09$; $df = 4$; $P > 0.05$, respectively; Figure 7C, 7D).

CAR Effects on Miniature PSCs

In order to further examine whether there was a direct modulation by CAR of the spontaneous neurotransmitter release process at the presynaptic level, we analyzed whether CAR could alter the frequency and amplitude of miniature PSCs recorded in the presence of TTX. Miniature EPSCs (inward currents) were more frequent than IPSCs (outward currents) at HP of -50 mV. Consequently, analysis in this condition was limited only to EPSCs. In SubCD neurons exhibiting an outward current in response to CAR application, there was a significant decrease in both frequency (1.1 ± 0.2 Hz Control vs. 0.7 ± 0.1 Hz CAR; $t = 3.19$; $df = 14$; $P < 0.01$; $n = 15$; Figure 7E) and amplitude (14.1 ± 1.0 pA Control vs. 13.1 ± 1.0 pA CAR; $t = 2.2$; $df = 14$; $P < 0.05$; $n = 15$; Figure 6A, 7F) of miniature EPSCs. Furthermore, the CAR-induced decrease in miniature EPSCs could be blocked by the application of MTO (Control = 0.54 ± 0.3 Hz; 16.3 ± 2.9 pA; CAR = 0.4 ± 0.3 Hz; 18.3 ± 4.9 pA; $n = 4$). These data suggest the presence of functional M2 receptors on presynaptic glutamatergic terminals projecting to SubCD neurons that exhibit an outward current in response to CAR. While cells exhibiting an inward current in response to CAR showed no significant changes in frequency of miniature EPSCs (Control = 1.9 ± 0.8 Hz; CAR = 2.0 ± 1.0 Hz; $n = 11$; $t = -0.48$; $df = 10$; $P > 0.05$), CAR did reduce the amplitude of these events (Control = 15.6 ± 0.7 pA; CAR = 14.8 ± 0.7 pA; $n = 11$; $t = 3.13$; $df = 10$; $P < 0.05$, Figure 7E, 7F). These results suggest a differential cholinergic modulation of presynaptic terminals of SubCD neurons that exhibit inward current vs. those that exhibit outward current in response to CAR.

DISCUSSION

This work used several methods to attempt to demonstrate the differential effects of CAR on SubCD neurons, thus providing some insight into the cholinergic modulation of these putative REM sleep-related cells. While this study did not directly identify recorded neurons by transmitter type, it did establish that CAR increased GABAergic/glycinergic transmission in the majority of neurons in this area while it also inhibited glutamatergic transmission in the SubCD. CAR-induced inward currents were mediated by M1 and nicotinic receptors, whereas CAR-induced outward currents were mediated by M2 receptors. The presence of glycinergic IPSCs suggests an important role for glycine in also mediating inhibition in this area. Furthermore, several intrinsic properties of SubCD neurons were found to change during development. Despite these changes, the mechanisms regulating the effects of CAR appeared to be largely in place by the first postnatal week. Finally, this study corroborated the results of a recent study that found that GABAergic neurons in the SubCD of transgenic mice were depolarized by CAR.⁵³

Postsynaptic Responses to CAR

Our results indicated that roughly one-half of SubCD cells were depolarized and the other half hyperpolarized by CAR. The outward current was shown to be mediated by a potassium current that could be blocked with either BaCl_2 or by the M2

receptor antagonist, MTO (Figure 2). In contrast, both PRZ and MEC were necessary to completely block the inward current induced by CAR. The presumed nicotinic inward current that persisted in the presence of TTX and PRZ revealed a reversal potential around -45 mV. In contrast, no reversal potential was obtained for the presumed M1 receptor-mediated current that remained in the presence of TTX and MEC. Some SubCD neurons with CAR-induced inward currents in control conditions exhibited a small outward current to CAR application in the presence of PRZ, MEC, and TTX. Previous studies have suggested that CAR may induce a biphasic effect on some extracellularly recorded neurons in the SubCD.⁵⁴ Therefore, it is possible that M2 receptors are co-localized with M1 and nicotinic receptors at least on some SubCD neurons, resulting in opposing CAR effects, leading to the observed variability in the reversal potentials of the CAR-induced currents. For example, the simultaneous activation of nicotinic receptors and the M2 receptor-mediated potassium conductance in the presence of TTX and PRZ may have led to the observed reversal potential of -45 mV, which was more negative than would be expected from a pure nicotinic receptor-induced current (0 mV).⁵⁵

Evoked EPSCs in the SubCD were consistently reduced by the application of CAR. This decrease in amplitude of evoked EPSCs could be blocked with muscarinic antagonists (Figure 5E). Furthermore, CAR induced an increase in the PPR without a concomitant change in evoked EPSC half-width. These data suggested the presence of presynaptic muscarinic receptors on glutamatergic terminals within this region. PHY, an acetylcholinesterase inhibitor, also decreased the amplitude of evoked EPSCs, suggesting that the spontaneous release of acetylcholine within the slice could mimic the inhibitory effects of CAR on these cells. Additionally, CAR significantly decreased the frequency of miniature EPSCs in the presence of TTX in some neurons. This provides further support for the presence of presynaptic muscarinic receptors on at least some glutamatergic terminals within the SubCD.

While CAR consistently inhibited spontaneous, miniature, and evoked EPSCs, there was some variation in the effects of CAR depending on the type of EPSCs investigated. CAR had a mainly inhibitory effect on evoked EPSCs while only cells exhibiting an outward current responded to CAR with a decrease in spontaneous or miniature EPSCs. This discrepancy between the effects of CAR on spontaneous and miniature EPSCs vs. evoked EPSCs is likely attributable to the differential activation of numerous glutamatergic terminals with evoked stimulation vs. the involvement of a likely much smaller population of activated terminals in producing spontaneous and miniature EPSCs. While it is premature to speculate about the precise origins of the glutamatergic inputs that were depressed by CAR, it is clear that CAR did inhibit EPSCs in the majority of SubCD neurons.

There was also some discrepancy between the potentiating effects of CAR on spontaneous IPSCs and the lack of effect of CAR on evoked IPSCs. Evoked stimulation may activate a large portion of the afferent terminals of these neurons in the control condition and thus prevent further potentiation effects by CAR. Additionally, anatomical localization of muscarinic receptors in other regions of the CNS such as the hippocampus and the striatum revealed that a large portion of GABAergic interneurons contained presynaptic M2 but not M1 receptors.⁵⁶⁻⁵⁸ This differ-

ential distribution of muscarinic receptors may account for the differential effects of CAR on evoked and spontaneous IPSCs. The absence of excitatory presynaptic cholinergic receptors on GABAergic/glycinergic terminals could account for the failure to observe a CAR-induced potentiation with evoked stimulation. Additionally, the increase in spontaneous IPSCs by CAR generally occurred in a rhythmic fashion, suggesting that these were action potential-dependent events. Thus, the differential effects of CAR on evoked and spontaneous IPSC may reflect differential anatomical sites of action.

Shunting is a process whereby a decrease in neuronal input resistance attenuates incoming PSCs. In an effort to control for possible shunting effects of CAR, GDP- β -S, a G protein antagonist, was added to the intracellular solution, and MEC was added to the extracellular solution. In these conditions, CAR decreased the evoked EPSCs with no concomitant change in the input resistance (Figure 5F). Furthermore, Figure 7 shows that, in the presence of GBZ and STR, spontaneous EPSCs were significantly decreased in frequency but not amplitude. These data suggest that the observed decreases in EPSCs by CAR could not be solely attributed to shunting effects that result from opening postsynaptic conductances.

A decrease in EPSC amplitude was detected in the presence of TTX (Figure 7F). CAR may generate at least some shunting in these neurons. As cholinergic inputs to this area likely induce diffuse neuromodulation, it is plausible that these projections mediate their effects, in part, by decreasing neuronal input resistance and consequently attenuating incoming PSCs in some cells.⁵⁹

Physiological Significance

The SubCD consists of a population of neurons that are critical for the induction of REM sleep atonia as well as the initiation of PGO and rat P-waves associated with REM sleep.^{7,23,24} In the last few decades, the use of in vivo and in vitro techniques has produced significant evidence supporting the role of cholinergic brainstem nuclei in modulating the REM sleep state.^{10,11,60,61} Specifically, the PPN contains cholinergic "REM-on" neurons, and excitation of this region using pharmacological agents has been shown to induce increases in REM sleep signs.^{7,31,62-64} These cholinergic neurons have widespread projections throughout the brainstem, including the SubCD nucleus of the rat.^{7,13,14} It has been shown that at least in some preparations in vivo, microinjections of CAR into the SubCD can induce REM sleep and rat P-waves.^{22,54,65,66} This suggests that the ascending projections of the SubCD may be important in modulating REM sleep, putative memory consolidation and possibly brainstem and hippocampal theta rhythms.⁶⁷⁻⁶⁹

We hypothesize is that during REM sleep, putative cholinergic "REM-on" neurons facilitate SubCD neurons to produce the REM sleep signs of muscle atonia and the P-waves seen in the rat via differential pre- and postsynaptic effects on glutamatergic and GABAergic neurons. The excitation of presumed GABAergic neurons, coupled with the inhibition of presumed glutamate neurons by cholinergic input to the SubCD may: (a) set up a rhythmic oscillation, especially since some of neurons, possibly GABAergic, have been found to be electrically coupled,³² and (b) hyperpolarize glutamate neurons, some of which have low-threshold spikes, subsequently inducing rhythmic

bursting in this population. This rhythmic bursting may then be critical for the onset and maintenance of REM sleep and its signs. Additional studies are required to support this hypothesis, but the present results provide evidence for this effect.

The SubCD remains an important region of interest given its potential role in learning and memory. Recent evidence suggests that activation of this region enhances learning performance,⁶² while lesions of this region impair certain learning paradigms.²² The high-frequency bursting observed in relation to P-waves have been proposed as the endogenous equivalent of tetanic activation required for long-term potentiation.^{24,30} Additional research is needed to confirm the presence of such activation arising in the SubCD and its effects on hippocampal neurons, however, this promises to become an exciting area of research in the future.

Limitations and Conclusions

There are a number of limitations of these studies that should be discussed. First, slices do not have sleep-wake cycles, so that conclusions regarding in vivo controls need to be tempered until confirmed in such preparations. Second, while we limited the sampling region to a small area immediately anterior to the 7th nerve, the region into which CAR injections induce REM sleep signs could not be identified in the same animals. Third, the complex excitatory effects of CAR need further study in order to determine if other muscarinic receptors, e.g., M3, might also be involved. We should also note that nicotinic receptors desensitize rapidly while bath application of CAR is typically used, nevertheless, the specific nicotinic antagonist MEC did block a current remaining after PRZ, suggesting that some nicotinic action was probably prevented by the presence of MEC after addition of CAR. Because no experiments using low calcium were performed, we cannot address the possible presence of TTX-resistant presynaptic nicotinic receptor vs TTX-susceptible post-synaptic nicotinic receptors. On the other hand, the present study provides important insights into the functional role of the cholinergic input modulating SubCD network activity. We showed that CAR can differentially inhibit excitatory and excite inhibitory synaptic transmission in the SubCD by increasing GABAergic/glycinergic IPSCs and inhibiting evoked, spontaneous, and miniature glutamatergic EPSCs. This implies a forceful push especially towards GABAergic activation. Given the discovery of electrically coupled neurons, which are typically GABAergic in a number of areas in the brain,^{31,34} it will be of interest to determine if the cholinergic input to SubCD is geared towards inducing ensemble activity.

ACKNOWLEDGMENTS

This work was supported by F30 NS053163 (DH), DC06356 and DC07123 (AH), R01 NS20246 (EGR), and by core facilities of the Center for Translational Neuroscience supported by grant P20 RR20146.

DISCLOSURE STATEMENT

This was not an industry supported study. The authors have indicated no financial conflicts of interest.

REFERENCES

- Koban M, Swinson KL. Chronic REM-sleep deprivation of rats elevates metabolic rate and increases UCP1, gene expression in brown adipose tissue. *Am J Physiol Endocrinol Metab* 2005;289:E68-74.
- Ramm P, Frost BJ. Cerebral and local cerebral metabolism in the cat during slow wave and REM sleep. *Brain Res* 1986;365:112-24.
- Rechtschaffen A, Bergmann BM. Sleep deprivation in the rat: an update of the 1989, paper. *Sleep* 2002;25:18-24.
- Roffwarg HP, Muzio JN, Dement WC. Ontogenetic development of the human sleep-dream cycle. *Science* 1966;152:604-19.
- Smith C. Sleep states and memory processes. *Behav Brain Res* 1995;69:137-45.
- Aserinsky E, Kleitman N. Regularly occurring periods of eye motility, and concomitant phenomena, during sleep. *Science* 1953;118:273-4.
- Datta S, Siwek DF, Patterson EH, Cipolloni PB. Localization of pontine PGO wave generation sites and their anatomical projections in the rat. *Synapse* 1998;30:409-23.
- Morrison AR. Paradoxical sleep without atonia. *Arch Ital Biol* 1988;126:275-89.
- Yamamoto K, Mamelak AN, Quattrochi JJ, Hobson JA. A cholinergic desynchronized sleep induction zone in the anterodorsal pontine tegmentum: locus of the sensitive region. *Neuroscience* 1990;39:279-93.
- Steriade M, Datta S, Pare D, Oakson G, Curro Dossi RC. Neuronal activities in brain-stem cholinergic nuclei related to tonic activation processes in thalamocortical systems. *J Neurosci* 1990;10:2541-59.
- Steriade M, Pare D, Datta S, Oakson G, Curro Dossi R. Different cellular types in mesopontine cholinergic nuclei related to pontogeniculo-occipital waves. *J Neurosci* 1990;10:2560-79.
- Imon H, Ito K, Dauphin L, McCarley RW. Electrical stimulation of the cholinergic laterodorsal tegmental nucleus elicits scopolamine-sensitive excitatory postsynaptic potentials in medial pontine reticular formation neurons. *Neuroscience* 1996;74:393-401.
- Mitani A, Ito K, Hallanger AE, Wainer BH, Kataoka K, McCarley RW. Cholinergic projections from the laterodorsal and pedunculopontine tegmental nuclei to the pontine gigantocellular tegmental field in the cat. *Brain Res* 1988;451:397-402.
- Shiromani PJ, Armstrong DM, Gillin JC. Cholinergic neurons from the dorsolateral pons project to the medial pons: a WGA-HRP and choline acetyltransferase immunohistochemical study. *Neurosci Lett* 1988;95:19-23.
- Gerber U, Stevens DR, McCarley RW, Greene RW. Muscarinic agonists activate an inwardly rectifying potassium conductance in medial pontine reticular formation neurons of the rat in vitro. *J Neurosci* 1991;11:3861-7.
- Greene RW, Gerber U, McCarley RW. Cholinergic activation of medial pontine reticular formation neurons in vitro. *Brain Res* 1989;476:154-9.
- Reese NB, Garcia-Rill E, Skinner RD. The pedunculopontine nucleus--auditory input, arousal and pathophysiology. *Prog Neurobiol* 1995;47:105-33.
- Stevens DR, Birnstiel S, Gerber U, McCarley RW, Greene RW. Nicotinic depolarizations of rat medial pontine reticular formation neurons studied in vitro. *Neuroscience* 1993;57:419-24.
- Jones BE. Immunohistochemical study of choline acetyltransferase-immunoreactive processes and cells innervating the pontomedullary reticular formation in the rat. *J Comp Neurol* 1990;295:485-514.
- Jouvet M, Jeannerod M, Delorme F. [Organization of the system responsible for phase activity during paradoxical sleep]. *C R Seances Soc Biol Fil* 1965;159:1599-604.
- Sanford LD, Morrison AR, Mann GL, Harris JS, Yoo L, Ross RJ. Sleep patterning and behaviour in cats with pontine lesions creating REM without atonia. *J Sleep Res* 1994;3:233-40.
- Mavanji V, Ulloor J, Saha S, Datta S. Neurotoxic lesions of phasic pontine-wave generator cells impair retention of 2-way active avoidance memory. *Sleep* 2004;27:1282-92.
- Datta S, Patterson EH, Siwek DF. Brainstem afferents of the cholinergic pontine wave generation sites in the rat. *Sleep Res Online* 1999;2:79-82.
- Datta S, MacLean RR. Neurobiological mechanisms for the regulation of mammalian sleep-wake behavior: reinterpretation of historical evidence and inclusion of contemporary cellular and molecular evidence. *Neurosci Behav Rev* 2007;31:775-824.
- Verret L, Leger L, Fort P, Luppi PH. Cholinergic and noncholinergic brainstem neurons expressing Fos after paradoxical (REM) sleep deprivation and recovery. *Eur J Neurosci* 2005;21:2488-504.
- Boissard R, Gervasoni D, Schmidt MH, Barbagli B, Fort P, Luppi PH. The rat ponto-medullary network responsible for paradoxical sleep onset and maintenance: a combined microinjection and functional neuroanatomical study. *Eur J Neurosci* 2002;16:1959-73.
- Bandyopadhyaya RS, Datta S, Saha S. Activation of pedunculopontine tegmental protein kinase A: a mechanism for rapid eye movement sleep generation in the freely moving rat. *J Neurosci* 2006;26:8931-42.
- Datta S, Mavanji V, Patterson EH, Ulloor J. Regulation of rapid eye movement sleep in the freely moving rat: local microinjection of serotonin, norepinephrine, and adenosine into the brainstem. *Sleep* 2003;26:513-20.
- Brown RE, Winston S, Basheer R, Thakkar MM, McCarley RW. Electrophysiological characterization of neurons in the dorsolateral pontine rapid-eye-movement sleep induction zone of the rat: intrinsic membrane properties and responses to carbachol and orexins. *Neuroscience* 2006;143:739-55.
- Datta S. Activation of phasic pontine-wave generator: a mechanism for sleep-dependent memory processing. *Sleep Biol Rhythms* 2006;4:16-26.
- Garcia-Rill E, Heister DS, Ye M, Charlesworth A, Hayar A. Electrical coupling: novel mechanism for sleep-wake control. *Sleep* 2007;30:1405-14.
- Heister DS, Hayar A, Charlesworth A, Yates C, Zhou YH, Garcia-Rill E. Evidence for electrical coupling in the subcoeruleus (SubC) nucleus. *J Neurophysiol* 2007;97:3142-7.
- Jouvet-Mounier D, Astic L, Lacote D. Ontogenesis of the states of sleep in rat, cat, and guinea pig during the first postnatal month. *Dev Psychobiology* 1970;2:216-39.
- Garcia-Rill E, Charlesworth A, Heister DS, Ye M, Hayar A. The developmental decrease in REM sleep: the role of transmitters and electrical coupling. *Sleep* 2008;31:673-90.
- Good CH, Bay KD, Buchanan R, Skinner RD, Garcia-Rill E. Muscarinic and nicotinic responses in the developing pedunculopontine nucleus (PPN). *Brain Res* 2007;1129:147-55.
- Kunitake A, Kunitake T, Stewart M. Differential modulation by carbachol of four separate excitatory afferent systems to the rat subiculum in vitro. *Hippocampus* 2004;14:986-99.
- Wada E, Waka K, Boulter J, et al. Distribution of alpha2, alpha3, alpha4, and beta2, neuronal nicotinic receptor subunit mRNAs in the central nervous system: a hybridization histochemical study in the rat. *J Comp Neurol* 1989;284:314-35.
- Seguela P, Wadiche J, Dineley-Miller K, Dani J, Patrick J. Molecular cloning, functional properties, and distribution of rat brain $\alpha 7$: a nicotinic cation channel highly permeable to calcium. *J Neurosci* 1993;13:596-604.
- Tibollet E, Bertrand D, Marquerat A, Raggenbass M. Comparative distribution of nicotinic receptor subtypes during development, adulthood and aging: an autoradiographic study in the rat brain. *Neuroscience* 2004;124:405-20.

40. Chavez-Noriega L, Crona J, Washburn M, Urrutia A, Elliott K, Johnson E. Pharmacological characterization of recombinant human neuronal nicotinic acetylcholine receptors h alpha 2, beta 2, h alpha 2, beta 4, h alpha 3, beta 2, h alpha 3, beta 4, h alpha 4, beta 2, h alpha 4, beta 4, and h alpha 7, expressed in *Xenopus* oocytes. *J Pharmacol Exp Ther* 1997;280:346-56.
41. Nabekura J, Murata O, Ishibashi H, Akaike N. Use-dependent suppression of the nicotinic acetylcholine receptor response by the proadrenomedullin N-terminal 20-amino acid peptide in rat locus coeruleus neurons. *J Neurochem* 1998;70: 865-70.
42. Masuda N, Hayashi Y, Matsuyoshi H, Chancellor MB, de Groat WC, Yoshimura N. Characterization of hyperpolarization-activated current (I_h) in dorsal root ganglion neurons innervating rat urinary bladder. *Brain Res* 2006;1096:40-52.
43. Roberts L, Greene JR. Hyperpolarization-activated current (I_h): a characterization of subicular neurons in brain slices from socially and individually housed rats. *Brain Res* 2005;1040:1-13.
44. Alreja M, Aghajanian GK. Pacemaker activity of locus coeruleus neurons: whole-cell recordings in brain slices show dependence on cAMP and protein kinase A. *Brain Res* 1991;556:339-43.
45. Williams JT, North RA, Shefner SA, Nishi S, Egan TM. Membrane properties of rat locus coeruleus neurones. *Neuroscience* 1984;13:137-56.
46. Dietz S, Murthy V. Contrasting short-term plasticity at two sides of the mitral-granule reciprocal synapse in the mammalian olfactory bulb. *Journal of Physiology* 2005;569: 475-88.
47. Paxinos G, Watson C. *The rat brain in stereotaxic coordinates*. 2nd ed. Orlando, FL: Academic Press, 1986.
48. Nunez A, De la Roza C, Rodrigo-Angulo M, Buno W, Reinoso-Suarez F. Electrophysiological properties and cholinergic responses of rat ventral oral pontine reticular neurons in vitro. *Brain Res* 1997;754:1-11.
49. Debanne D, Guerineau NC, Gahwiler BH, Thompson SM. Paired-pulse facilitation and depression at unitary synapses in rat hippocampus: quantal fluctuation affects subsequent release. *J Physiol* 1996;491:163-76.
50. Manabe T, Wyllie DJ, Perkel DJ, Nicoll RA. Modulation of synaptic transmission and long-term potentiation: effects on paired pulse facilitation and EPSC variance in the CA1, region of the hippocampus. *J Neurophysiol* 1993;70:1451-9.
51. Hayar A, Heyward PM, Heinbockel T, Shipley MT, Ennis M. Direct excitation of mitral cells via activation of alpha1-noradrenergic receptors in rat olfactory bulb slices. *J Neurophysiol* 2001;86:2173-82.
52. Hsu KS, Yang CH, Huang CC. Carbachol induces inward current in rat neostriatal neurons through a G-protein-coupled mechanism. *Neurosci Lett* 1997;224:79-82.
53. Brown RE, McKenna JT, Winston S, et al. Characterization of GABAergic neurons in rapid-eye-movement sleep controlling regions of the brainstem reticular formation in GAD67-green fluorescent protein knock-in mice. *Eur J Neurosci* 2008;27:352-63.
54. Hayar A, Heister DS, Garcia-Rill E. Carbachol induces synchronization of IPSCs at theta frequency in whole-cell recorded Subcoeruleus neurons. *Sleep* 2007;30:A35.
55. Bordey A, Feltz P, Trouslard J. Nicotinic actions on neurones of the central autonomic area in rat spinal cord slices. *J Physiol* 1996;497:175-87.
56. Calabresi P, Centonze D, Gubellini P, Pisani A, Bernardi G. Acetylcholine-mediated modulation of striatal function. *Trends Neurosci* 2000;23:120-6.
57. Hernandez-Echeagaray E, Galarraga E, Bargas J. 3-Alpha-chloro-imperialine, a potent blocker of cholinergic presynaptic modulation of glutamatergic afferents in the rat neostriatum. *Neuropharmacology* 1998;37:1493-502.
58. Levey AI, Edmunds SM, Koliatsos V, Wiley RG, Heilman CJ. Expression of m1-m4, muscarinic acetylcholine receptor proteins in rat hippocampus and regulation by cholinergic innervation. *J Neurosci* 1995;15:4077-92.
59. Lucas-Meunier E, Fossier P, Baux G, Amar M. Cholinergic modulation of the cortical neuronal network. *Pflugers Arch* 2003;446:17-29.
60. Kubin L. Carbachol models of REM sleep: recent developments and new directions. *Arch Ital Biol* 2001;139:147-68.
61. McCarley RW. Mechanisms and models of REM sleep control. *Arch Ital Biol* 2004;142:429-67.
62. Datta S, Mavanji V, Ulloor J, Patterson EH. Activation of phasic pontine-wave generator prevents rapid eye movement sleep deprivation-induced learning impairment in the rat: a mechanism for sleep-dependent plasticity. *J Neurosci* 2004;24:1416-27.
63. Mitler MM, Dement WC. Cataplectic-like behavior in cats after micro-injections of carbachol in pontine reticular formation. *Brain Res* 1974;68:335-43.
64. Datta S, Siwek DF. Single cell activity patterns of pedunculopontine tegmentum neurons across the sleep-wake cycle in the freely moving rat. *J Neurosci Res* 2002;70:611-621.
65. Gnadt JW, Pegram GV. Cholinergic brainstem mechanisms of REM sleep in the rat. *Brain Res* 1986;384:29-41.
66. Mavanji V, Datta S. Activation of the phasic pontine-wave generator enhances improvement of learning performance: a mechanism for sleep-dependent plasticity. *Eur J Neurosci* 2003;17:359-70.
67. Karashima A, Katayama N, Nakao M. Phase-locking of spontaneous and tone-elicited pontine waves to hippocampal theta waves during REM sleep in rats. *Brain Res* 2007;1182:73-81.
68. Karashima A, Nakao M, Honda K, Iwasaki N, Katayama N, Yamamoto M. Theta wave amplitude and frequency are differentially correlated with pontine waves and rapid eye movements during REM sleep in rats. *Neurosci Res* 2004;50:283-9.
69. Lydic R, Douglas CL, Baghdoyan HA. Microinjection of neostigmine into the pontine reticular formation of C57BL/6J mouse enhances rapid eye movement sleep and depresses breathing. *Sleep* 2002;25:835-41.